DHX15 overexpression suppresses colorectal cancer cell line proliferation

YUKI II[1,2], KOSUKE SAITA[2], TOSHIRO IWAGAWA[2], SHINGO ITO[3], KIICHI SUGIMOTO[1], KAZUHIRO SAKAMOTO[1] and SUMIKO WATANABE[2]

[1]Department of Coloproctological Surgery, Juntendo University Graduate School of Medicine, Tokyo 113-8421, Japan; [2]Department of Retinal Biology and Pathology, Graduate School of Medicine, University of Tokyo, Tokyo 113-8655, Japan; [3]Department of Gastrointestinal Surgery, Shonan Kamakura General Hospital, Kanagawa 247-0072, Japan

Received April 30, 2025; Accepted October 20, 2025

DOI: 10.3892/ol.2025.15433

Abstract. DEAH (Asp-Glu-Ala-His) box helicase 15 (DHX15) is a member of the DEAD box RNA helicase family that carries out a key role in innate immunity against viral infections. It is involved in tumorigenesis as a tumor-promoting factor in various types of cancer, but it has also been suggested to act as a tumor suppressor. However, the role of DHX15 in colorectal cancer (CRC) remains largely unknown. In the present study, we examined the role of DHX15 in CRC. Immunostaining of clinical samples from patients with CRC identified DHX15 proteins in the cell nuclei of both tumor and adjacent normal tissues. DHX15 overexpression was revealed to reduce the cell number of various CRC cell lines, as well as the number of Ki67-positive proliferating cells. However, the number of AC3-positive apoptotic cells was comparable between the control and DHX15-overexpressing cells. The possible downstream mechanisms of DHX15 were further examined which revealed that activation of the Wnt/β-catenin and NF-κB signaling pathways were not affected by DHX15 expression. However, DHX15 overexpression resulted in fewer LC3 puncta in HCT116 and DLD1 cells. Taken together, DHX15 may negatively affect CRC cell proliferation, and autophagy may potentially be involved in the downstream mechanism of DHX15.

Correspondence to: Professor Sumiko Watanabe, Department of Retinal Biology and Pathology, Graduate School of Medicine, University of Tokyo, 7-3-1 Hongo, Bunkyo, Tokyo 113-8655, Japan
E-mail: sumiko@g.ecc.u-tokyo.ac.jp

Abbreviations: DHX15, DEAH (Asp-Glu-Ala-His) box helicase 15; CRC, colorectal cancer; IEC, epithelial cell; RT-qPCR, reverse transcription-quantitative PCR; TCF-luc, TCF-binding site luciferase; NFκB-luc, NF-κB binding sites luciferase

Key words: colorectal cancer, DHX15, cell proliferation, tumorigenesis, autophagy

Introduction

DEAH box helicase 15 (DHX15), which is a member of the DEAH box RNA helicase family (1), is involved in several cellular processes, such as splicing and ribosome biogenesis and facilitates remodeling of large RNA-protein complexes (2-4). DHX15 was shown to carry out a role in antiviral immune response *in vivo* (5). In RNA virus-induced intestinal inflammation, DHX15 carries out a pivotal role in controlling inflammation by sensing IFN-β and other cytokines produced by RNA viruses (6). Moreover, DHX15 is reported to be involved in tumorigenesis as a tumor-promoting factor in acute lymphoblastic leukemia and cancer of the lung, prostate or breast (7-10), but it also acts as a tumor suppressor in hepatocellular carcinoma and gastric cancer (11,12). Using gain- and loss-of-function analyses, we previously revealed that DHX15 suppressed the proliferation of glioma cell lines (13).

Colorectal cancer (CRC) is the third most common type of cancer, with ~2 million cases diagnosed worldwide in 2020, and the second most common cause of cancer-related mortality, according to the International Agency for Research on Cancer of the World Health Organization (14). Repeat analyses of public single-cell sequence and bulk transcriptome data revealed consistent upregulation of DHX15 expression in patients with CRC (15-17). Analysis of the clinical pathological features of CRC samples from the Cancer Gene Atlas and the Clinical Proteomic Tumor Analysis Consortium revealed that reduced expression of *DHX15* mRNA and DHX15 protein associated with poor CRC prognosis in terms of survival, metastasis and recurrence (16). Furthermore, the overall survival positively associated with DHX15 expression levels in CRC (18). Conversely, in a case report of a patient with CRC harboring a KRAS p.G12D mutation, DHX15 was implicated as a critical mediator of microbiota-driven pathogenesis of CRC. Specifically, DHX15 was found to be highly expressed and functioned as a receptor on tumor cells, facilitating the invasion of *Fusobacterium nucleatum* into the nuclei of intestinal epithelial cells (IECs), thereby promoting tumorigenesis (19). The present study examined the effects of DHX15 overexpression using CRC cell lines with different characteristics, including *KRAS* mutations (19).

Materials and methods

Human clinical samples. Human CRC samples and adjacent normal tissues were obtained by surgical resection from ten patients with CRC; five male, average age 60 years (51-65 years), five female, average age 75.6 years (60-91 years) at Juntendo University Hospital (Tokyo, Japan) between April 2022-August 2025 and embedded in paraffin. The diagnoses of the ten patients were based on clinical and pathological examinations (Table I). Cancer staging was carried out in accordance with the Union for International Cancer Control TNM classification (20). All human tissues were obtained with written informed consent and approval from the medical ethical committee of Juntendo University Hospital (Tokyo, Japan; approval no. E22-0079).

Reagents, CRC cell lines, transfection and cell sorting. Porcupine inhibitor C59 (cat. no. S7037) was obtained from Selleck Chemicals and the NF-κB inhibitor IMD-0354 (cat. no. HY-10172) was obtained from MedChemExpress. The human CRC cell lines HCT116 (21), SW480 (22) and Caco2 (23) (provided by Dr Akira Orimo, Juntendo University, Tokyo, Japan) were cultured in low glucose DMEM (Nacalai Tesque, Inc.) and DLD1 cells (24) (provided by Dr Akira Orimo, Juntendo University, Tokyo, Japan) were cultured in RPMI1640 (Nacalai Tesque, Inc.); both culture media were supplemented with 10% FBS (MilliporeSigma) and penicillin-streptomycin (MilliporeSigma). The characteristics of the four CRC cell lines are summarized in (Table SI) (25).

HCT116, SW480, Caco2 and DLD1 cells ($1.5x10^6$ cells) were seeded on 10-cm plates (Nippon Gene Co., Ltd.) and transfected using GeneJuice Transfection Reagent (Cat. no. 70967-3CN; Merck KGaA) with a combination of the plasmids pMXs-IP (control vector) or pMX-DHX15 and EGFP expression (pCAG-EGFP), at DNA amounts of 0.03 μg for pCAG-EGFP and 0.21 μg for pMXs-IP or pMX-DHX15 per well. The cells were harvested at 37˚C after 12 h of culture and EGFP-positive cells were collected using a cell sorter (FACS ARIA III, BD Biosciences). Total RNA was purified using Trizol® reagent (Thermo Fisher Scientific, Inc.).

Quantitative reverse transcription PCR (RT-qPCR). RT-qPCR was carried out as previously described (26). The expression levels of the transcripts of interest were normalized using *GAPDH* and *ACTB* values. The respective forward and reverse primer sequences were as follows: human *ACTB*: 5'-GAAGGAGATCACTGCCCTGG-3' and 5'-ACTCCTGCTTGCTGATCCAC-3'; *GAPDH*: 5'-ATTGCCCTCAACGACCACTT-3' and 5'-TGGTCCAGGGGTCTTACTCC-3'; *DHX15*: 5'-TGCTGAACGTCTACCATGCTT-3' and 5'-ATTCGAGATAGCTGCTGGCG-3'; *IRF1*: 5'-AAGGGGTGTGGCCTTTTTAGA-3' and 5'-TGTCCCTGTTCACCCCAAAG-3'; *IRF3*: 5'-CCTGCACATTTCCAACAGCC-3' and 5'-AATCCATGCCCTCCACCAAG-3': *IRF7*: 5'-GCTCCCCACGCTATACCATC-3' and 5'-CAGGGAAGACACACCCTCAC-3'; *NFKB1*: 5'-GTGAAGACCACCTCTCAGGC-3' and 5'-CTGTCGCAGACACTGTCACT-3'; *NFKB2*: 5'-ACGCCTCTTGACCTCACTTG-3' and 5'-GTGGCTCCATGGTGTTCTGA-3'; *RELA*: 5'-GGACATGGACTTCTCAGCCC-3' and 5'-AAAGTTGGGGGCAGTTGGAA-3'; and *REL*: 5'-TCCTTAGCCCAGCCATCTCT-3' and 5'-GGCAGTCTCCGCTCATCTTT-3'.

Immunohistochemistry. DHX15 protein expression in human clinical samples was examined by immunohistochemistry using an anti-DDX15 antibody (H-4, 1:500; Santa Cruz Biotechnology; cat. no. sc-271686). Paraffin-embedded 3-μm sections were first deparaffinized with EZ Prep (cat. no. 950-102) and subjected to antigen retrieval using Cell Conditioner #2 (pH 9.0; cat. no. 950-223) on a BenchMark Ultra automated stainer (Roche Tissue Diagnostics). After antigen retrieval, the sections were incubated with the primary anti-DDX15 antibody at 37˚C for 1 h.

Primary antibody signals were then detected using the UltraView Universal DAB Detection Kit (Roche Tissue Diagnostics, cat. no. 760-500) under standard BenchMark Ultra settings, including an 8-min incubation with the HRP-conjugated multimer reagent, followed by DAB chromogen visualization. Counterstaining was performed with Hematoxylin II for 8 min and Bluing Reagent for 4 min at 37˚C. Stained sections were observed using a Zeiss Axio Imager M2 fluorescence microscope (Zeiss GmbH), and images were acquired using ZEN software (version 3.12; Zeiss GmbH).

Stained samples were observed using Zeiss Axio Imager M2 fluorescence microscope (Zeiss GmbH) and images were acquired using ZEN software (ZEN3.12; Zeiss GmbH). For quantification of DHX15 positive signals, we used ImageJ (version 1.54p; National Institutes of Health). The images were imported to ImageJ and DAB signals were isolated using the color deconvolution command of ImageJ. DAB images were converted to gray scale binary images, and doublet cells were separated by the Watershed command and positive and negative cells were counted. To quantify intensity of the signals, the log10 value of mean of sample ROI vs. mean of background ROI by using 8-bit index color was calculated.

Immunohistochemistry of the cultured cells was carried out as described previously (27). The primary antibodies used were mouse monoclonal antibodies against Ki67 (1:250; cat. no. 55060; BD); LC3 (1:2,000; cat. no. M152-3; MEDICAL & BIOLOGICAL LABORATORIES CO., LTD.); rabbit polyclonal antibody against active Caspase-3 (AC3; 1:250; cat. no. 9664S; Promega Corporation); and chicken polyclonal antibody against GFP (1:2,000; cat. no. ab13970; Abcam). Appropriate secondary antibodies conjugated with Alexa Fluor 488 (1:500; cat. no. A11039; Thermo Fisher Scientific, Inc.) or Alexa Fluor 594 (1:500; cat. no. C10639; Thermo Fisher Scientific, Inc.) were used. The nuclei were visualized using DAPI. Stained cells were observed using Zeiss Axio Imager I fluorescence microscope (Zeiss GmbH) and images were acquired using ZEN software (version, 3.12; Zeiss GmbH).

Luciferase reporter assay for Wnt/β-catenin and NF-κB signaling pathways. Luciferase reporter assays for the Wnt/β-catenin and NF-κB signaling pathways were performed using TCF-luc (IFN minimal promoter with 7x TCF-binding sites driving firefly luciferase) and NFκB-luc (SV40 early promoter with 8x NF-κB-binding sites driving firefly luciferase) (28). These plasmids were kindly provided by Dr. K. Shimotono (Kyoto University, Kyoto, Japan) and Dr. R. Tsuruta (University of Tokyo, Tokyo, Japan), respectively.

Table I. DHX15 expression in human CRC tissues and clinicopathological factors of the patients with CRC.

Patient	Age (years)	Sex	Location	Stage	T	N	M	Histological type	V	Ly	DHX15 immuno-Histochemical staining: Adjacent tissue	DHX15 immuno-Histochemical staining: Cancer
1	75	W	C	IIIc	4a	2b	0	por	0	1c	48	58
2	62	M	A	IIIb	3	1a	0	tub2	1c	0	34	56
3	82	W	A	IIIb	3	2a	0	tub2	1a	1c	17	74
4	60	W	T	IIIb	3	1b	0	tub1	0	1a	47	76
5	51	M	T	II	3	0	0	tub1	0	1a	35	49
6	91	W	S	IIIb	3	1a	0	tub2	1b	1a	36	77
7	65	M	S	IIIc	4a	3	0	tub2	0	1a	21	59
8	60	M	S	II	3	0	0	tub1	1a	0	14	48
9	62	M	RS	IIa	3	0	0	tub1	0	0	29	57
10	70	W	RS	II	3	0	0	tub2	1c	1a	49	69

V, vascular invasion; Ly, lymphatic invasion; A. ascending colon; T, transverse colon; S, sigmoid colon; RS, rectal sigmoid colon; Tub1, well differentiated adenocarcinoma; Tub2, moderate differentiated adenocarcinoma; Tub1, Por, poorly differentiated adenocarcinoma; W, women; M, male; DHX15, DEAH (Asp-Glu-Ala-His) box helicase 15.

No 3' UTR reporter constructs and no miRNA mimics or inhibitors were used in this study. Cells were transfected with the reporter plasmids using GeneJuice Transfection Reagent (cat. no. 70967-3CN; MilliporeSigma) according to the manufacturer's instructions. Luciferase activity was measured 18 h after transfection using a luminometer (Lumat LB9507; Titertek-Berthold) and the Luciferase Assay System (Promega, cat. no. E1500). Because only firefly luciferase reporters were used, luciferase activity was analyzed without Renilla luciferase normalization.

Cell proliferation assay. SW480 ($1x10^4$cell/well), Caco2 ($1x10^4$ cell/well), HCT116 ($2x10^4$ cells) and DLD1 ($2x10^4$ cells) cells were plated on 48-well plates (Corning, Inc.) and then transfected with a combination of plasmids pMXs-IP (control vector) or pMX-DHX15 and pCAG-EGFP using GeneJuice (cat. no. 70967-3CN; MilliporeSigma). After 1 h of incubation, the plate was set on IncuCyte ZOOM (Sartorius AG). Live-cell images were captured every 8 h and analyzed using IncuCyte Live-Cell Imaging Software (v2024B).

To evaluate the time-dependent changes in the number of GFP-positive cells after transfection, cells were monitored using an Incucyte live-cell imaging system under standard culture conditions (37˚C; 5% CO_2) at 8-h intervals immediately after plating.

Cell proliferation was examined by incorporating 5-ethynyl 2'-deoxyuridine (EdU) using Click-iT EdU Alexa Fluor 594 Imaging kit (Thermo Fisher Scientific, Inc.). After transfecting the cells as aforementioned, EdU was added to the culture at a final concentration of 10 μM and incubated for 2 h at 37˚C. For inhibitor experiments, cells were treated with the Wnt inhibitor C59 (10 μM) or the NF-κB inhibitor IMD-0354 (5 μM) at 37˚C for 2 h prior to EdU addition. The incorporated EdU signals were visualized by immunostaining with a chicken polyclonal antibody against GFP (cat. no. ab13970; 1:2,000; Abcam) at room temperature overnight and a secondary antibody conjugated with Alexa Fluor 488 at room temperature for 30 min (1:500; Thermo Fisher Scientific, Inc.). EGFP was immunostained with an anti-GFP antibody (1:2,000; cat. no. ab13970; Abcam). Nuclei were stained with DAPI. Stained cells were observed using Zeiss Axio Imager I (Zeiss GmbH) and images were acquired using ZEN software (Zeiss GmbH).

Western blotting. Cell lysates were collected from cell lines ($2x10^6$ cells) and analyzed by western blotting, as previously described (29). Protein was extracted using RIPA buffer (Nacalai Tesque, Inc.), containing 50 mM Tris-HCl (pH 7.4), 150 mM NaCl, 1% NP-40, 0.5% sodium deoxycholate and 0.1% SDS, supplemented with protease inhibitor cocktail (Nacalai Tesque, Inc.).

Protein concentration was determined using the BCA assay (Nacalai Tesque, Inc..) according to the manufacturer's protocol. Equal amounts of protein (3 μg per lane) were mixed with 4x Laemmli sample buffer (Nacalai Tesque, Inc.) and boiled at 98˚C for 5 min before electrophoresis. Proteins were separated on 10% SDS-PAGE gels. Proteins were transferred onto PVDF membranes. Membranes were blocked in 5% non-fat dry milk (Bio-Rad) in TBS-Tween (0.1%) at room temperature for 1 h. Membranes were incubated with primary antibodies at 4˚C overnight, followed by incubation with HRP-conjugated secondary antibodies for 1 h at room temperature. Signals were detected using Chemi-Lumi One Super (Nacalai Tesque, Inc.). The primary antibodies used were mouse monoclonal antibodies against ACTIN (1:1,000; cat. no. A4700; MilliporeSigma) and DDX15 (1:1,000; cat. no. sc-271686; Santa Cruz Biotechnology, Inc.). The secondary antibody used was HRP-linked secondary antibodies (1:5,000; cat. no. NA931; Cytiva).

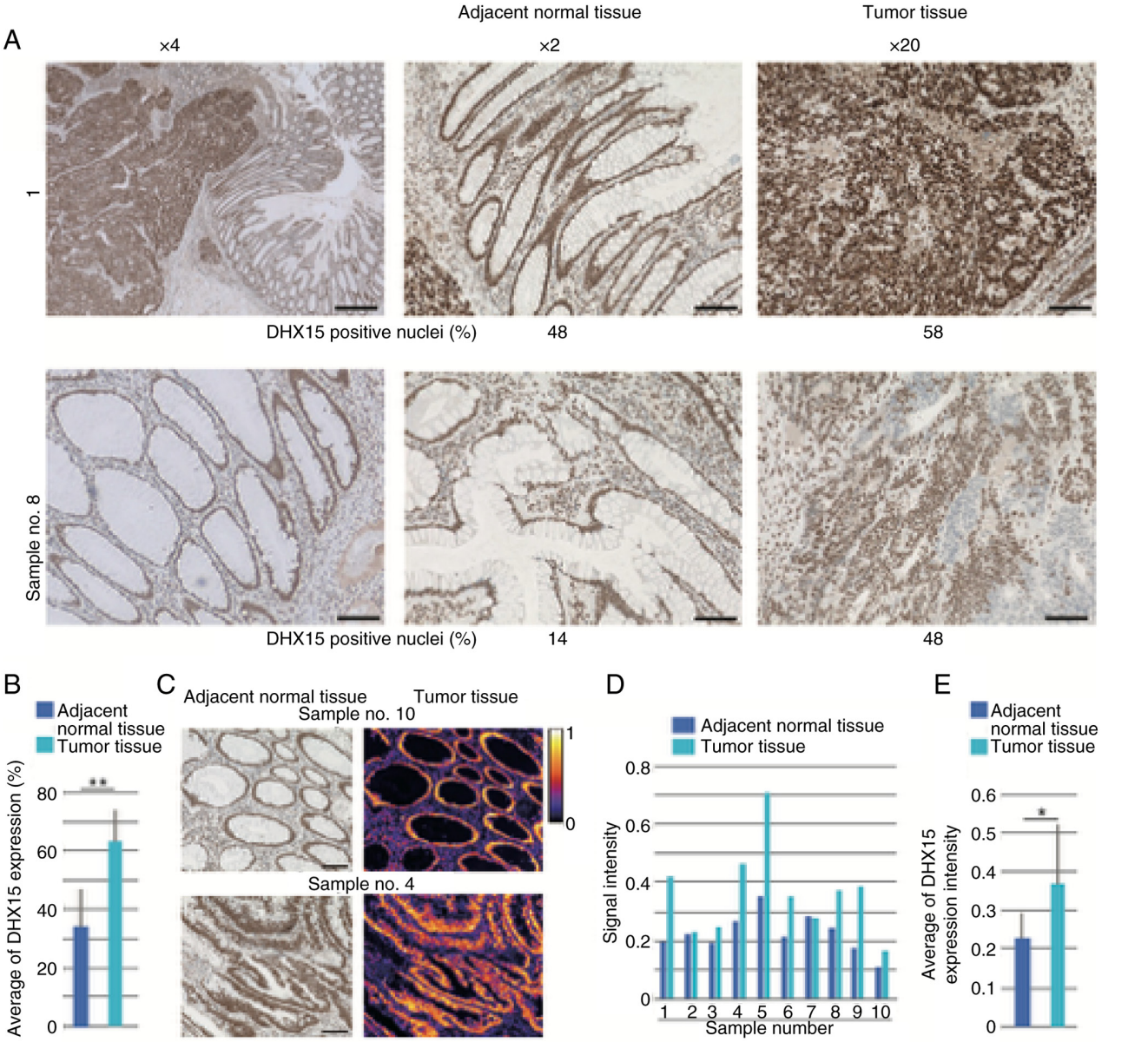

Figure 1. DHX15 immunohistochemistry of human CRC clinical samples. (A) Representative images of tumor and adjacent normal tissue. DHX15 expression in tumor and adjacent non-tumor tissues was examined by immunohistochemistry. Evaluation of expression strength was carried out using ImageJ and percentage of positive signals are shown in the bottom of the panel. (B) Average of DHX15 signal-positive nuclei population of normal and tumor tissues of 10 samples. (C) Representative images of examination of intensity of DHX15 staining signals. Left panels are imuunostained patterns and right panels are converted to 8-bit color index. (D) Signal intensity of adjacent normal tissues and tumor tissues of the 10 samples. (E) Average DHX15 signal intensity of normal and tumor tissues of 10 samples. Scale bars represent 100 μm in A and C. *P<0.01; **P<0.01. DHX15, DEAH (Asp-Glu-Ala-His) box helicase 15.

Statistical analysis. Statistical significance was calculated by an unpaired Student's t test (two tailed). P<0.05 was considered to indicate a statistically significant difference; *P<0.05, **P<0.01. Experiments were conducted in triplicate. Data are shown as mean ± standard deviation)

Results

DHX15 expression in human CRC tissues. On examination of the clinical samples, DHX15 protein was detectable in the cell nuclei in both tumor and adjacent normal tissues of all 10 patients (Fig. 1A). The evaluation values of DHX15 expression strength for all 10 samples are summarized (Table I). The average positive nuclei staining of DHX15 in the ten tumor samples was increased compared with that of adjacent tissue (Fig. 1B). Among the CRC tissues, four showed >60% of DHX15 positive signals in tumor tissues, but there was no correlation between clinicopathological factors and DHX15 staining intensity (Table I). Heat-map (Fig. 1C) represents intensity of DHX15 immunostaining of adjacent normal tissue and tumor tissue (Fig. 1D). Again, clear association between pathological observation and signal intensity was not found, but the average DHX15 expression intensity in the tumor region was increased compared with that in adjacent tissue (Fig. 1E).

Effects of DHX15 overexpression on the proliferation of CRC cell lines. DHX15 protein expression levels were first examined in the CRC cell lines HCT116, SW480, Caco2 and DLD1 using

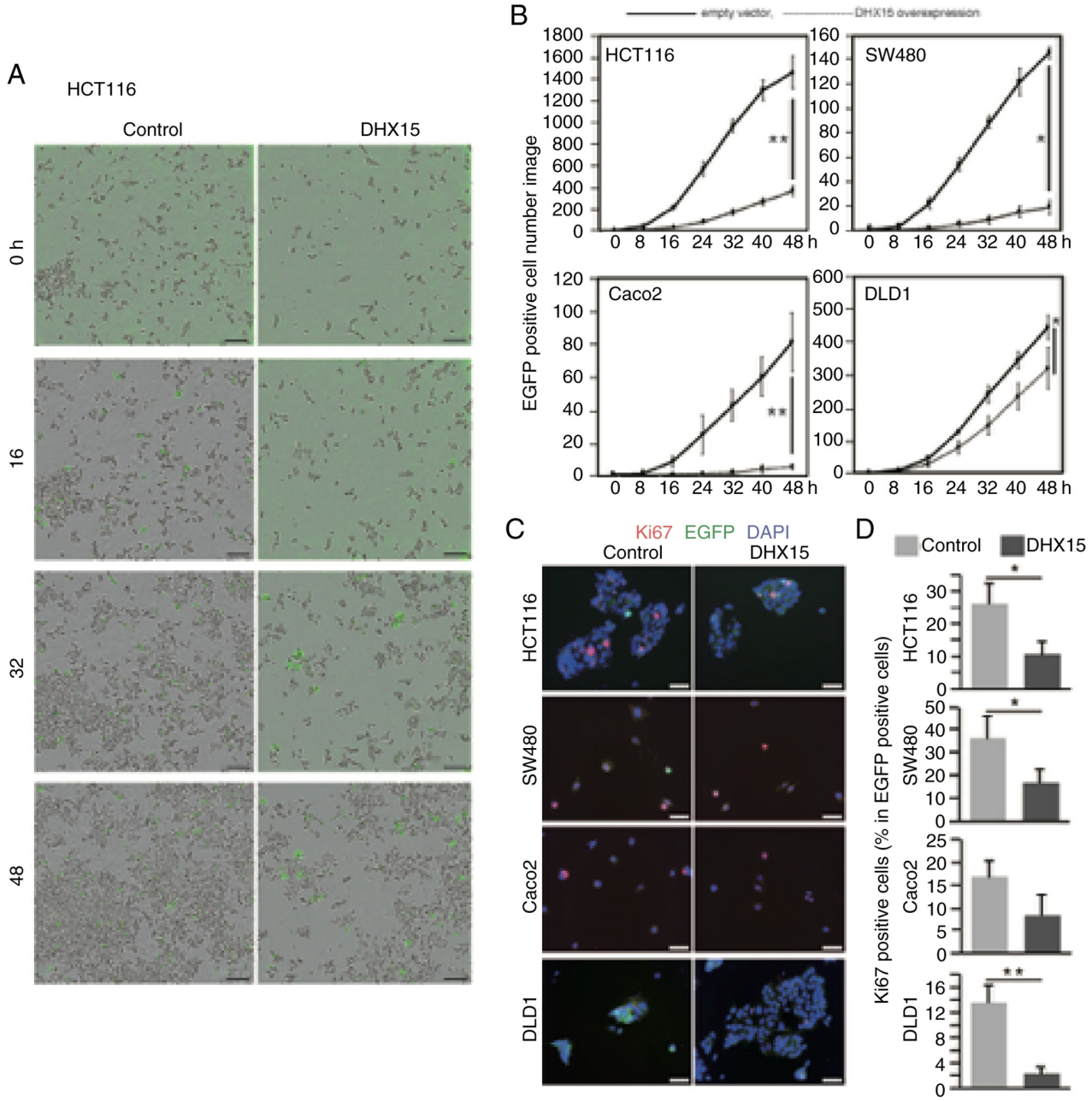

Figure 2. Effects of DHX15 overexpression on the proliferation of various CRC cell lines. The CRC cell lines HCT116, SW480, Caco2 and DLD1 were transfected with DHX15-expressing or empty vector with EGFP-expressing vector. The cells were incubated in IncuCyte ZOOM, and live-cell images were captured every 8 h. (A) The population of EGFP positive cells was analyzed using IncuCyte Live-Cell Imaging Software. The captured images of HCT116 of control and DHX15 overexpressed cells at 0, 16, 32 and 48 h after transfection. (B) Transition of number of EGFP positive cells from 0 to 48 h after transfection of empty vector or DHX15 overexpression vector. Cell proliferation was examined by Ki67 immunostaining. Transfected cells were cultured for 24 h, followed by immunostaining with an anti-Ki67 antibody. (C) Representative images, DAPI (blue) shows nucleus. (D) Population of Ki67 positive cells in total EGFP positive cells in the 4 cell lines. Scale bar, 100 μm in A and C. Data are average of 3 independent samples with SEM. Statistical significance was calculated by Student's t test (two tailed). *P<0.01; **P<0.01. DHX15, DEAH (Asp-Glu-Ala-His) box helicase 15; CRC, colorectal cancer.

western blotting of whole protein. All cell lines express DHX15 with expected size (Fig. S1A; upper bands). Subsequently, the cells were co-transfected with DHX15-expression vector or empty control vector together with EGFP-expression plasmid and EGFP positive cells were purified by a cell sorter after 12 h of culture. Overexpression of *DHX15* transcripts was confirmed by RT-qPCR in all four cell lines (Fig. S1B).

To examine the effects of DHX15 overexpression on proliferation, the cells were cotransfected with DHX15-expressing vector or empty control vector with EGFP-expression plasmid. The transfected cells were cultured for 2 days, and the number of EGFP-positive cells was counted over time using IncuCyte live-cell imaging. The number of EGFP-positive cells is shown on Fig. 2A and B. Compared with the control samples, samples with DHX15 overexpression had a significantly reduced cell number in all the examined CRC cell lines (Fig. 2B). These results suggested that DHX15 suppressed cell proliferation.

The number of Ki67-positive proliferating HCT116, SW480 and DLD1 cells was significantly reduced after transfection with DHX15 and EGFP-expression plasmid (Fig. 2C and D).

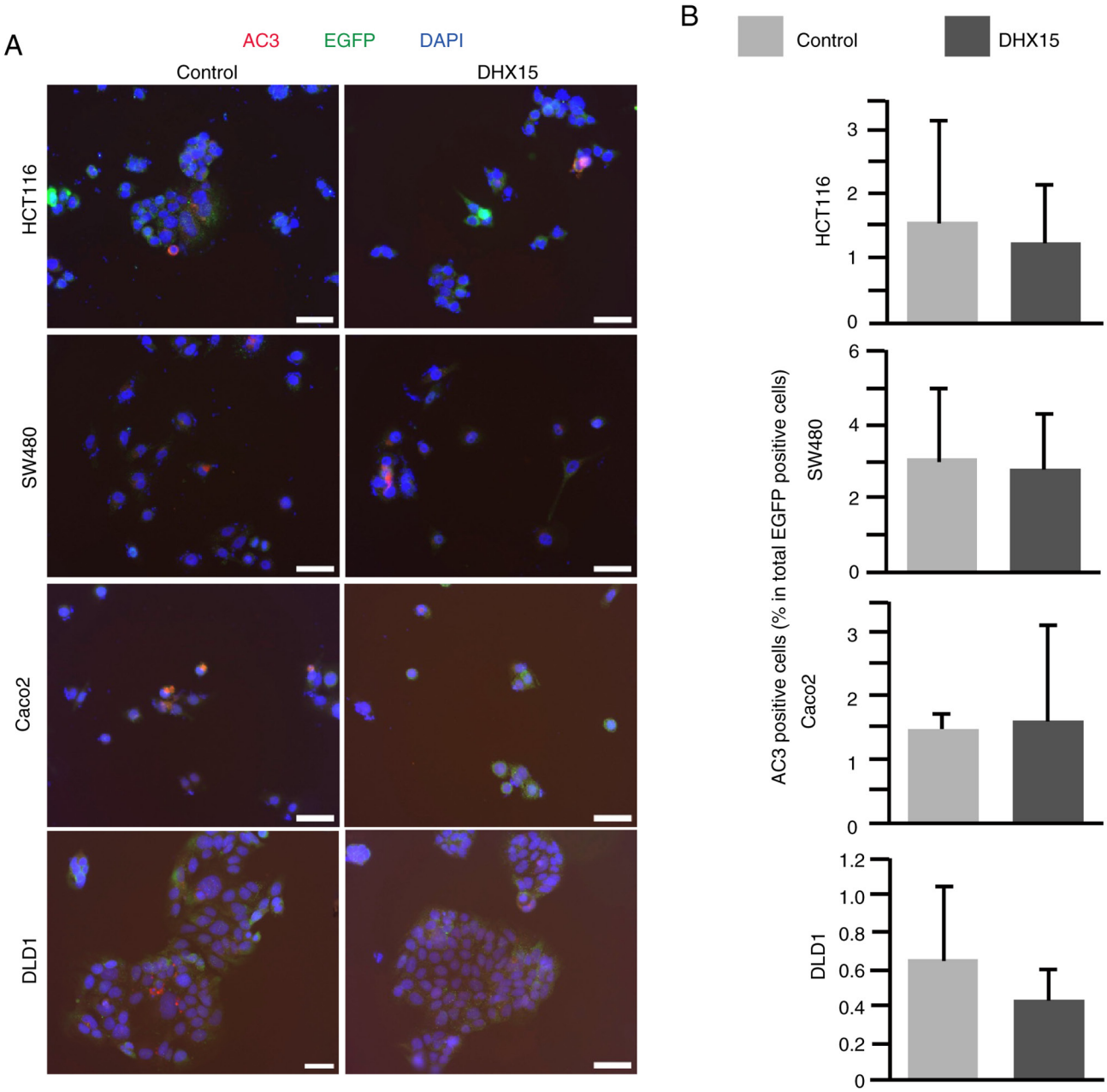

Figure 3. Effects of DHX15 overexpression on CRC cells line apoptosis. Apoptosis of the DHX15-overexpressing CRC cell lines was examined using active Caspase-3 (AC3) immunostaining. Transfected cells were cultured 24 h and immunostaining with anti-AC3 antibody was carried out. DAPI (blue) shows nucleus. (A) Representative images of each sample. (B) Population of AC3 positive cells in total EGFP positive cells in the 4 cell lines. Scale bar, 100 μm in A. Data are average of 3 independent samples with SEM. Statistical significance was calculated by Student's t test (two tailed), all comparison were P>0.05 (B). DHX15, DEAH (Asp-Glu-Ala-His) box helicase 15; CRC, colorectal cancer.

The EdU incorporation assay revealed that DHX15 overexpression significantly reduced the number of EdU-positive cells in all four CRC cell lines (Fig. S2A and B). These results suggested that DHX15 suppressed the proliferation of CRC cell lines.

Next, the DHX15-overexpressing CRC cell lines were investigated using the immunohistochemistry apoptosis marker AC3. The cells were cotransfected with either the empty control or DHX15-expressing vector with EGFP-expression plasmid and immunostaining was carried out after 2 days of culture. The number of AC3-positive apoptotic cells was comparable between the control and DHX15-transfected cells in the four CRC cell lines, except HCT116, which showed slight decrease in AC3-positive cells in the DHX15 overexpression group, although this was not significant (Fig. 3A and B). These results indicated that DHX15 overexpression may not affect apoptosis in the CRC cell lines.

Examination of the possible involvement of Wnt, NF-κB and autophagy in DHX15-overexpressing cells. To investigate the potential mechanisms underlying this finding, the involvement of the Wnt and NF-κB signaling pathways were examined, as well as autophagy, in DHX15-overexpressing cells. These pathways have previously been reported to play key roles in the regulation of cell proliferation (11,30,31). Analysis revealed that DHX15 overexpression significantly induced

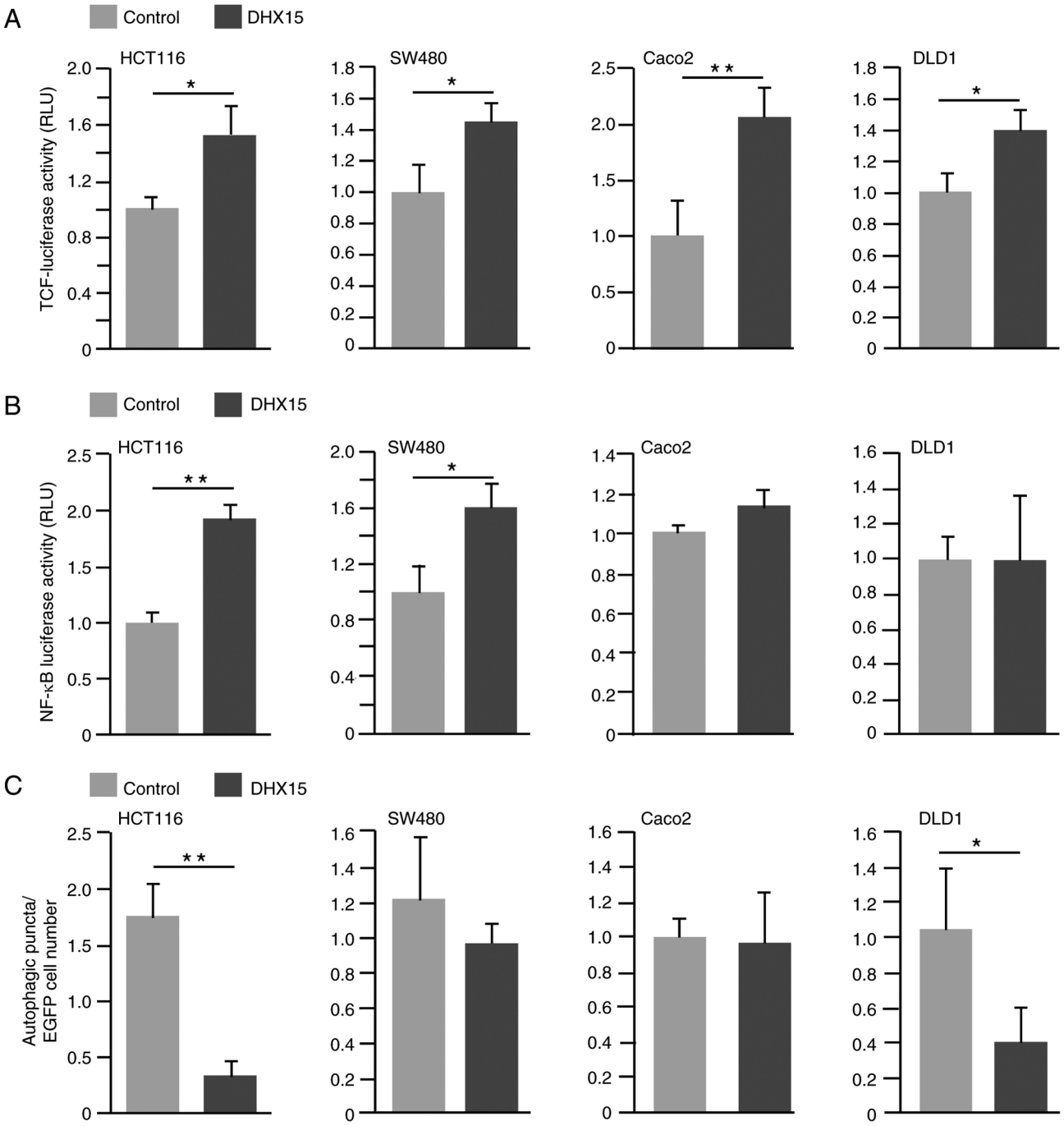

Figure 4. Effects of DHX15 overexpression on the activation of Wnt, NF-κB and autophagy. CRC cell lines were transfected with DHX15 or vector control with luciferase reporter plasmids to detect Wnt and NF-κB activities and then harvested after 18 h of incubation. CRC cell lines were transfected with DHX15 or vector control with EGFP-expression plasmids and then immunostained with anti-LC3 antibody after 8 h of culture. Luciferase activities of each (A) TCF-luc or (B) NF-κB-luc cell line. (C) The number of LC3-positive puncta signals among all EGFP-positive cell lines. Data are average of 3 independent samples with SEM. Statistical significance was calculated by Student's t test (two tailed). *P<0.01; **P<0.01. DHX15, DEAH (Asp-Glu-Ala-His) box helicase 15; CRC, colorectal cancer.

luciferase activities that were dependent on the TCF-binding motif in all examined CRC cells (Fig. 4A). The effects of the Wnt signaling inhibitor C59 on the proliferation of CRC cell lines with overexpressed DHX15 were investigated using EdU incorporation assay. Analysis revealed a tendency for higher EdU incorporation in HCT116 and SW480 cells when compared with control cells (Fig. S3A and B).

On examination of NF-κB signaling using a NF-κB target site-dependent luciferase assay, DHX15 overexpression enhanced luciferase activity in HCT116 and SW480 cells; however, in Caco2 and DLD1 cells, luciferase activity was similar between the control and DHX15-overexpressing cells (Fig. 4B). On examination of NF-κB-related gene expression by RT-qPCR in HCT116 and SW480 cells, the control and DHX15-overexpressing cells revealed similar transcript levels of genes, except for *IRF3* and *REL* in SW480 cells (Fig. S4). Examination of the effects of the NF-κB inhibitor IMD-0354 revealed that the number of EdU-positive cells

was not significantly different between DHX15-transfected and IMD-0354 treated cells in all four CRC cell lines (Fig. S5A and B).

The expression pattern of LC3 puncta, which is an autophagy marker (32), was subsequently examined. Upon counting the LC3-positive puncta in the nuclei of control and DHX15-overexpressing cells, DHX15 overexpression led to a reduced number of LC3-positive signals in HCT116 and DLD1 cells but not in SW480 and Caco2 cells (Figs. 4C and S6).

Discussion

The present study investigated the role of DHX15 in CRC by examining DHX15 expression levels in clinical samples and changes in DHX15 levels in CRC cell lines. In the clinical samples from 10 patients with CRC, DHX15 expression levels varied. The absence of a clear association between clinicopathological factors and intensity of DHX15 expression was likely attributable to the small sample size (n=10 patients). Further analysis of DHX15 expression using additional clinical samples may help clarify its relationship with clinicopathological factors. Although the relationship between DHX15 expression levels and tumor malignancy remains inconclusive, the quantification of its expression may provide a potential prognostic indicator, such as recurrence or reduced survival in cases with low DHX15 expression. At present, to the best of our knowledge, no association has been observed between DHX15 expression and tumor stage. In addition, we hypothesize that there is a possibility that the DHX15 expression patterns and levels are associated with disease progression which may be revealed by monitoring the condition of patients continuously and carefully. Conversely, analysis revealed that DHX15 upregulation hampered the proliferation activity of all examined CRC cell lines. This result is consistent with a recent study which revealed that DHX15 inhibits CRC progression, invasion and metastasis (18). In the present study, all CRC cell lines examined exhibited endogenous DHX15 expression. Therefore, further forced overexpression of DHX15 may have exceeded the physiological threshold, leading to cytotoxicity. Such supraphysiological expression levels could disrupt essential cellular processes, ultimately resulting in growth suppression. Mutation in the well-known protooncogene *KRAS* is found in HCT116, SW480 and DLD1 cell lines but not in Caco2 cells; therefore, the DHX15 effects observed in the present study were likely not associated with *KRAS* mutation. However, evaluation of DHX15 protein expression patterns and their relationship with clinicopathological factors in hepatocellular carcinoma revealed that DHX15 was markedly upregulated, and its high expression associated with poor prognosis (33). Taken together with the reports of other types of cancer, we hypothesize that the effects on DHX15 expression levels to cancer prognosis depend on the types of cancer.

Among the various mechanisms of DHX15 activity, Wnt involvement has been reported in different model systems. In one study that analyzed the role of DHX15 in antibacterial responses in IECs, mice with *DHX15* deletion in IECs were susceptible to infection with enteric bacteria because of low levels of α defensin, which is an antimicrobial peptide; considering that α defensin is induced by the TLR/Wnt pathways this study suggested that DHX15 regulates TLR/Wnt signals (34). Another study revealed that DHX15 regulates zebrafish intestinal development through the Wnt signaling pathway (35). The present study revealed that DHX15 overexpression significantly induced Wnt signaling in the four CRC cell lines; however, inhibition of Wnt signaling did not prevent the suppressed proliferation of DHX15-overexpressing cells. Furthermore, given its well-known contribution to the development and progression of various tumors (36,37), Wnt signaling was less likely to participate in the suppression of cell proliferation by DHX15. However, other physiological processes, such as metastasis, were not analyzed in the present study and requires *in vivo* clarification in future research.

DHX15 acts as an immune modulator through regulation of NF-κB. Human DHX15 contributes to activation of the NF-κB, JNK and p38 MAPK pathways in HeLa cells in response to the synthetic double-stranded RNA analog poly(I:C) (5). In acute myeloid leukemia, DHX15 is downregulated in disease remission or cell line differentiation (7). Furthermore, knockdown of *DHX15* inhibits nuclear translocation and activation of the NF-κB subunit P65 in leukemia cells (7). Positive feedback of NF-κB and DHX15 was reported in breast cancer cells (10). The present study revealed that DHX15 overexpression induced NF-κB signaling in HCT116 and SW480 cells, but the expression levels of known downstream target genes of the NF-κB pathway were not upregulated. Furthermore, NF-κB inhibition by the IMD-0354 did not affect cell proliferation, suggesting the need to clarify the signaling pathways and biological roles of DHX15 using cell lines in the future.

Involvement of autophagy in cancer progression has been reported in various types of cancer (38-41). DHX15 negatively regulates autophagy in association with mTORC1 activation in hepatoma cells (11). There have been several reports on *KRAS*-activating mutations and autophagy. *KRAS*-activating mutations increase autophagy and contribute to the survival of CRC cells under starvation conditions (42). In addition, autophagy was induced to different degrees, depending on mutations of the *KRAS* allele (42). In the present study, given the decreased number of LC3 puncta in HCT116 and DLD1 cells, which have a $KRAS^{G13D/-}$ mutation, a relationship between *KRAS* mutation and autophagy was suspected. However, the contribution of this pathway to cell proliferation remains unclear. The effects of other signaling pathway inhibitors were also explored using this experimental model (data not shown). Preliminary experiments were performed with various inhibitor concentrations, and cell proliferation was assessed by EdU immunostaining. No significant differences were observed between the groups. However, because the efficacy of the inhibitor itself was not fully confirmed, these data are not included in the present study. Experiments in which knockdown of DHX15 is achieved by siRNA oligonucleotide are planned as future work.

Although the present study did not yield fully conclusive mechanistic results, it provides novel evidence that DHX15 overexpression suppresses colorectal cancer cell proliferation and highlights DHX15 as a previously under-recognized regulator of tumor biology. These findings offer a foundation for future mechanistic studies and suggest that DHX15 may serve as a potential biomarker or therapeutic target in colorectal cancer.

Acknowledgements

The authors would like to thank Dr. Kanji Uchida (Department of Anesthesiology, University of Tokyo Hospital, Tokyo, Japan) for discussions and allowing the use of IncuCyte in their department.

Funding

No funding was received.

Availability of data and materials

The data generated in the present study are included in the figures and/or tables of this article.

Authors' contributions

YI and KoS performed the experiments, TI, SI, KoS, KiS, KaS and SW designed the research, YI and SW wrote the manuscript. SW contributed to the study conception, experimental design, data interpretation, and provided critical revisions of the manuscript. YI and SW confirm the authenticity of all the raw data. All authors read and approved the final manuscript.

Ethics approval and consent to participate

All human tissues were obtained with written informed consent and approval from the medical ethical committee of Juntendo University Hospital, Tokyo, Japan (approval no. E22-0079).

Patient consent for publication

Not applicable.

Competing interests

The authors declare that they have no competing interests.

References

1. Linder P: Dead-box proteins: A family affair-active and passive players in RNP-remodeling. Nucleic Acids Res 34: 4168-4180, 2006.
2. Arenas JE and Abelson JN: Prp43: An RNA helicase-like factor involved in spliceosome disassembly. Proc Natl Acad Sci USA 94: 11798-11802, 1997.
3. Combs DJ, Nagel RJ, Ares M Jr and Stevens SW: Prp43p is a DEAH-box spliceosome disassembly factor essential for ribosome biogenesis. Mol Cell Biol 26: 523-534, 2006.
4. Tanaka N, Aronova A and Schwer B: Ntr1 activates the Prp43 helicase to trigger release of lariat-intron from the spliceosome. Genes Dev 21: 2312-2325, 2007.
5. Mosallanejad K, Sekine Y, Ishikura-Kinoshita S, Kumagai K, Nagano T, Matsuzawa A, Takeda K, Naguro I and Ichijo H: The DEAH-box RNA helicase DHX15 activates NF-κB and MAPK signaling downstream of MAVS during antiviral responses. Sci Signal 7: ra40, 2014.
6. Xing J, Zhou X, Fang M, Zhang E, Minze LJ and Zhang Z: DHX15 is required to control RNA virus-induced intestinal inflammation. Cell Rep 35: 109205, 2021.
7. Pan L, Li Y, Zhang HY, Zheng Y, Liu XL, Hu Z, Wang Y, Wang J, Cai YH, Liu Q, *et al*: DHX15 is associated with poor prognosis in acute myeloid leukemia (AML) and regulates cell apoptosis via the NF-kB signaling pathway. Oncotarget 8: 89643-89654, 2017.
8. Yao G, Chen K, Qin Y, Niu Y, Zhang X, Xu S, Zhang C, Feng M and Wang K: Long non-coding RNA JHDM1D-AS1 interacts with DHX15 protein to enhance non-small-cell lung cancer growth and metastasis. Mol Ther Nucleic Acids 18: 831-840, 2019.
9. Jing Y, Nguyen MM, Wang D, Pascal LE, Guo W, Xu Y, Ai J, Deng FM, Masoodi KZ, Yu X, *et al*: DHX15 promotes prostate cancer progression by stimulating Siah2-mediated ubiquitination of androgen receptor. Oncogene 37: 638-650, 2018.
10. Zheng W, Wang X, Yu Y, Ji C and Fang L: CircRNF10-DHX15 interaction suppressed breast cancer progression by antagonizing DHX15-NF-κB p65 positive feedback loop. Cell Mol Biol Lett 28: 34, 2023.
11. Zhao M, Ying L, Wang R, Yao J, Zhu L, Zheng M, Chen Z and Yang Z: DHX15 inhibits autophagy and the proliferation of hepatoma cells. Front Med (Lausanne) 7: 591736, 2020.
12. Zong Z, Li H, Ning Z, Hu C, Tang F, Zhu X, Tian H, Zhou T and Wang H: Integrative bioinformatics analysis of prognostic alternative splicing signatures in gastric cancer. J Gastrointest Oncol 11: 685-694, 2020.
13. Ito S, Koso H, Sakamoto K and Watanabe S: RNA helicase DHX15 acts as a tumour suppressor in glioma. Br J Cancer 117: 1349-1359, 2017.
14. Sung H, Ferlay J, Siegel RL, Laversanne M, Soerjomataram I, Jemal A and Bray F: Global cancer statistics 2020: GLOBOCAN estimates of incidence and mortality worldwide for 36 cancers in 185 countries. CA Cancer J Clin 71: 209-249, 2021.
15. Lv X, Ma W, Miao X, Hu S and Xie H: Navigating colorectal cancer prognosis: A Treg-related signature discovered through single-cell and bulk transcriptomic approaches. Environ Toxicol 39: 3512-3522, 2024.
16. Lu P, Zhang Y, Cui Y, Liao Y, Liu Z, Cao ZJ, Liu JE, Wen L, Zhou X, Fu W and Tang F: Systematic characterization of full-length RNA isoforms in human colorectal cancer at single-cell resolution. Protein Cell 16: 873-895, 2025.
17. Tao Y, Li J, Pan J, Wang Q, Ke RW, Yuan D, Wu H, Cao Y and Zhao L: Integration of scRNA-Seq and bulk RNA-Seq identifies circadian rhythm disruption-related genes associated with prognosis and drug resistance in colorectal cancer patients. Immunotargets Ther 14: 475-489, 2025.
18. Fan L, Guo X, Zhang J, Wang Y, Wang J and Li Y: Relationship between DHX15 expression and survival in colorectal cancer. Rev Esp Enferm Dig 115: 234-240, 2023.
19. Zhu H, Li M, Bi D, Yang H, Gao Y, Song F, Zheng J, Xie R, Zhang Y, Liu H, *et al*: Fusobacterium nucleatum promotes tumor progression in KRAS p.G12D-mutant colorectal cancer by binding to DHX15. Nat Commun 15: 1688, 2024.
20. Huang SH and O'Sullivan B: Overview of the 8th edition TNM classification for head and neck cancer. Curr Treat Options Oncol 18: 40, 2017.
21. Rajput A, Martin ID, Rose R, Beko A, Levea C, Sharratt E, Mazurchuk R, Hoffman RM, Brattain MG and Wang J: Characterization of HCT116 human colon cancer cells in an orthotopic model. J Surg Res 147: 276-281, 2008.
22. Verhagen MP, Xu T, Stabile R, Joosten R, Tucci FA, van Royen M, Trerotola M, Alberti S, Sacchetti A and Fodde R: The SW480 cell line as a model of resident and migrating colon cancer stem cells. iScience 27: 110658, 2024.
23. Sambuy Y, De Angelis I, Ranaldi G, Scarino ML, Stammati A and Zucco F: The Caco-2 cell line as a model of the intestinal barrier: Influence of cell and culture-related factors on Caco-2 cell functional characteristics. Cell Biol Toxicol 21: 1-26, 2005.
24. Dexter DL, Spremulli EN, Fligiel Z, Barbosa JA, Vogel R, VanVoorhees A and Calabresi P: Heterogeneity of cancer cells from a single human colon carcinoma. Am J Med 71: 949-956, 1981.
25. Ahmed D, Eide PW, Eilertsen IA, Danielsen SA, Eknæs M, Hektoen M, Lind GE and Lothe RA: Epigenetic and genetic features of 24 colon cancer cell lines. Oncogenesis 2: e71, 2013.
26. Saita K, Moriuchi Y, Iwagawa T, Aihara M, Takai Y, Uchida K and Watanabe S: Roles of CSF2 as a modulator of inflammation during retinal degeneration. Cytokine 158: 155996, 2022.
27. Koso H, Yi H, Sheridan P, Miyano S, Ino Y, Todo T and Watanabe S: Identification of RNA-binding protein LARP4B as a tumor suppressor in glioma. Cancer Res 76: 2254-2264, 2016.
28. Tsuruta L, Lee HJ, Masuda ES, Yokota T, Arai N and Arai K: Regulation of expression of the IL-2 and IL-5 genes and the role of proteins related to nuclear factor of activated T cells. J Allergy Clin Immunol 96: 1126-1135, 1995.

29. Kuribayashi H, Iwagawa T, Murakami A, Kawamura T, Suzuki Y and Watanabe S: NMNAT1 is essential for human iPS cell differentiation to the retinal lineage. Invest Ophthalmol Vis Sci 65: 37, 2024.
30. Kabiri Z, Greicius G, Zaribafzadeh H, Hemmerich A, Counter CM and Virshup DM: Wnt signaling suppresses MAPK-driven proliferation of intestinal stem cells. J Clin Invest 128: 3806-3812, 2018.
31. Jiao L, Jiang M, Liu J, Wei L and Wu M: Nuclear factor-kappa B activation inhibits proliferation and promotes apoptosis of vascular smooth muscle cells. Vascular 26: 634-640, 2018.
32. Levine B and Kroemer G: Biological functions of autophagy genes: A disease perspective. Cell 176: 11-42, 2019.
33. Xie C, Liao H, Zhang C and Zhang S: Overexpression and clinical relevance of the RNA helicase DHX15 in hepatocellular carcinoma. Hum Pathol 84: 213-220, 2019.
34. Wang Y, He K, Sheng B, Lei X, Tao W, Zhu X, Wei Z, Fu R, Wang A, Bai S, *et al*: The RNA helicase Dhx15 mediates Wnt-induced antimicrobial protein expression in Paneth cells. Proc Natl Acad Sci USA 118: e2017432118, 2021.
35. Yao J, Cai Y, Chen Z, Wang X, Lai X, Pan L, Li Y and Wang S: Dhx15 regulates zebrafish intestinal development through the Wnt signaling pathway. Genomics 115: 110578, 2023.
36. Yu F, Yu C, Li F, Zuo Y, Wang Y, Yao L, Wu C, Wang C and Ye L: Wnt/β-catenin signaling in cancers and targeted therapies. Signal Transduct Target Ther 6: 307, 2021.
37. Ge X and Wang X: Role of Wnt canonical pathway in hematological malignancies. J Hematol Oncol 3: 33, 2010.
38. Chang SH, Huang SW, Wang ST, Chung KC, Hsieh CW, Kao JK, Chen YJ, Wu CY and Shieh JJ: Imiquimod-induced autophagy is regulated by ER stress-mediated PKR activation in cancer cells. J Dermatol Sci 87: 138-148, 2017.
39. Russell RC and Guan KL: The multifaceted role of autophagy in cancer. EMBO J 41: e110031, 2022.
40. Jalali P, Shahmoradi A, Samii A, Mazloomnejad R, Hatamnejad MR, Saeed A, Namdar A and Salehi Z: The role of autophagy in cancer: From molecular mechanism to therapeutic window. Front Immunol 16: 1528230, 2025.
41. Niu X, You Q, Hou K, Tian Y, Wei P, Zhu Y, Gao B, Ashrafizadeh M, Aref AR, Kalbasi A, *et al*: Autophagy in cancer development, immune evasion, and drug resistance. Drug Resist Updat 78: 101170, 2025.
42. Alves S, Castro L, Fernandes MS, Francisco R, Castro P, Priault M, Chaves SR, Moyer MP, Oliveira C, Seruca R, *et al*: Colorectal cancer-related mutant KRAS alleles function as positive regulators of autophagy. Oncotarget 6: 30787-30802, 2015.